Atmos. Chem. Phys. Discuss., 14, 8915–8961, 2014
www.atmos-chem-phys-discuss.net/14/8915/2014/
doi:10.5194/acpd-14-8915-2014

Atmospheric Chemistry and Physics Discussions

Analysis of nucleation events in the European boundary layer using the regional aerosol-climate model REMO-HAM with a solar radiation-driven OH-proxy

J.-P. Pietikäinen[1], S. Mikkonen[2], A. Hamed[2,†], A. I. Hienola[1], W. Birmili[3], M. Kulmala[4], and A. Laaksonen[1,2]

[1]Finnish Meteorological Institute, P.O. Box 503, 00101 Helsinki, Finland
[2]Department of Applied Physics, University of Eastern Finland, P.O. Box 1627, 70211 Kuopio, Finland
[3]Leibniz Institute for Tropospheric Research (IfT), Permoserstr. 15, 04318 Leipzig, Germany
[4]Department of Physics, University of Helsinki, P.O. Box 44, 00014, Helsinki, Finland
[†]deceased in September 2013

Received: 13 January 2014 – Accepted: 25 March 2014 – Published: 2 April 2014

Correspondence to: J.-P. Pietikäinen (joni-pekka.pietikainen@fmi.fi)

Published by Copernicus Publications on behalf of the European Geosciences Union.

ACPD
14, 8915–8961, 2014

Abstract

This work describes improvements in the regional aerosol-climate model REMO-HAM in order to simulate more realistically the process of atmospheric new particle formation (NPF). As a first modification, a new scheme was implemented to simulate OH radical concentrations, now using a proxy approach based on observations and also accounting for the effects of clouds upon OH concentrations. Second, the nucleation rate calculation was modified to directly simulate the formation rates of 3 nm particles, which removes some unnecessary steps in formation rate calculations used earlier in the model. Using the updated model version, the NPF over Europe was simulated for the comprehensive periods 2003–2004 and 2008–2009. The statistics of the simulated particle formation events were subsequently compared to observations from 13 ground-based measurement sites. The new model shows improved agreement with the observed NPF rates compared to former versions and can simulate the event statistics realistically for most parts of Europe. It is our conclusion that further modifications of the OH proxy that reflect the diverse atmospheric composition across Europe have the potential to further improvements.

1 Introduction

Atmospheric aerosols influence our quality of life in many different ways, from affecting human health and diminishing visibility, to changing the climate patterns and the hydrological cycle. An important phenomenon associated with the atmospheric aerosol system is the formation of new aerosol particles through gas-to-particle conversion, a process that seems to occur almost everywhere in the atmosphere (Kulmala et al., 2004). The atmospheric relevance of the nucleation is undisputed: it strongly influences the aerosol number concentration and makes an important contribution to local cloud condensation nuclei (CCN) concentrations (Lihavainen et al., 2003; Kerminen et al.,

ACPD
14, 8915–8961, 2014

2005; Laaksonen et al., 2005). As such, nucleation is among the key processes that need to be represented in state-of-the-art regional and global aerosol-climate models.

Modelling nucleation and the subsequent growth is a difficult task. Based on the assumption that sulphuric acid (H_2SO_4) is the main driving force in the process of nucleation, several parametrizations have been proposed to explain NPF: binary water–sulphuric acid nucleation (Vehkamäki et al., 2002), ternary water–sulphuric acid–ammonia nucleation (Napari et al., 2002; Merikanto et al., 2007), ion-induced nucleation involving water and sulphuric acid (Modgil et al., 2005), and combined neutral and ion-induced nucleation (Kazil and Lovejoy, 2007), as well as two nucleation parametrizations for the forested boundary layer (BL) – the cluster activation mechanism (Kulmala et al., 2006; Sihto et al., 2006) and the kinetic mechanism (Laakso et al., 2004; Kuang et al., 2008). These parametrizations are designed to rapidly estimate the number of nucleated particles as a function of the main controlling parameter (H_2SO_4) at the expense of severely reducing the complexity of the process.

The ability of global and regional models to predict NPF events has been tested before. Spracklen et al. (2008) used a global aerosol microphysics model, GLOMAP, to predict the contribution of boundary layer nucleation to regional and global distributions of CCN. They found that, by using the cluster activation scheme, the modelled particle size distribution and total particle number concentration at three continental sites in Europe was improved. Makkonen et al. (2009) modified the global climate model ECHAM5-HAM with respect to NPF by including several optional nucleation parametrizations that could be run together with binary homogeneous sulphuric acid–water nucleation. By adding the cluster activation parametrization to the boundary layer, the authors found that the particle number concentration in the lower atmosphere increased more than ten-fold, while in the upper atmosphere the increase was even larger. The study shows also that the cloud droplet number concentration in ECHAM5-HAM depends on the nucleation mechanism used. Kazil et al. (2010) implemented a new scheme for neutral and ion-induced nucleation of sulphuric acid and water in the global aerosol climate model ECHAM5-HAM, considering that such a nucleation

ACPD
14, 8915–8961, 2014

mechanism is a good candidate to explain NPF over the oceans and free troposphere. The nucleation via cluster activation, which requires the presence of organics, was used only for the forested boundary layer. The combination of these parametrizations seemed to better explain the observations than the cluster activation alone.

Many other studies using global aerosol-climate models have demonstrated the importance of atmospheric NPF for regional and global aerosol number concentration and cloud condensation nuclei budgets (Merikanto et al., 2009; Pierce et al., 2007; Pierce and Adams, 2009; Wang and Penner, 2009; Yu and Luo, 2009; Trivitayanurak et al., 2008; Jung et al., 2010; Laakso et al., 2013), each author having his/her own nucleation parametrization of choice. However, as global models have a large grid size (usually 200–300 km when aerosols are included), predicting the changes in the number concentration of newly formed particles and in size distribution is prone to large uncertainties. In this respect, regional climate models seem to be more appropriate for this mission.

Numerous regional climate models exist, but only a few have been used to analyse NPF. Sotiropoulou et al. (2006) used the air quality model UAM-AERO to study the impact of NPF on regional air quality and CCN formation. They concluded that an online coupled regional aerosol-climate model would improve the nucleation analysis done in their work. Matsui et al. (2011) used the regional climate model WRF-chem to study NPF over the Beijing region in China. The authors showed that the model is able to reproduce the timing of NPF and find non-NPF days. Matsui et al. (2011) reported that reductions in primary aerosol emissions do not necessarily lead to lower CCN concentrations because NPF tends to cancel out the effect of reductions. Fountoukis et al. (2012) used a three dimensional chemical transport model with microphysical model PMCAMx-UF by Jung et al. (2010) to simulate NPF on a European scale. Fountoukis et al. (2012) showed that, regionally, the total particle number concentrations can be increased by a factor of 3 when nucleation is included. Based on their results, a semi-empirical ternary sulphuric acid–ammonia–water parameterization performs better than kinetic or activation parameterization.

ACPD
14, 8915–8961, 2014

In this study, the predictive capability of the NPF of the regional aerosol-climate model REMO-HAM is investigated. The results are compared with measurements from 13 European sites. REMO-HAM is modified in this work to include a new measurement-based OH-proxy. The advantage thereof is that the incoming solar radiation is linked to the OH concentrations, thus taking into account the effects of clouds. In addition, the particle formation rate from clusters is replaced by the direct formation of 3 nm particles via H_2SO_4 condensation. Also, the old kinetic nucleation scheme only calculates the nucleation at forested boundary layer. The new approach removes this limitation and the nucleation is now calculated in all grid boxes.

The article is structured as follows: first, the models with their modifications and the methods are described in Sect. 2; Sect. 3 presents a detailed analysis of the results, followed by Sect. 4, where the main conclusions are listed and further steps are discussed.

2 Methods

2.1 Model description

2.1.1 ECHAM5-HAM global aerosol-climate model

In this work, the updated version ECHAM5-HAM2 (Roeckner et al., 2003; Stier et al., 2005; Zhang et al., 2012) is used to provide lateral aerosol boundary data for the regional model simulations. ECHAM-HAM2 is a global aerosol-climate model that includes the updated HAM2 aerosol module (Stier et al., 2005; Zhang et al., 2012) and the microphysical module M7 (Vignati et al., 2004).

2.1.2 REMO-HAM regional aerosol-climate model

In this study, the main tool is the regional aerosol-climate model REMO-HAM (Pietikäinen et al., 2012). The core of REMO-HAM is a hydrostatic, three-dimensional

ACPD
14, 8915–8961, 2014

atmosphere model developed at the Max Planck Institute for Meteorology in Hamburg, and is based on the Europa Model, the former numerical weather prediction model of the German Weather Service (Jacob and Podzun, 1996; Jacob, 2001). The physical core of REMO is based on the physical packages of the global circulation model ECHAM4 (Roeckner et al., 1996). Many parts of the model; for example, the cloud and soil treatments, have been updated (Pfeifer, 2003; Semmler et al., 2004; Hagemann, 2002; Rechid, 2009; Kotlarski, 2007). With respect to the aerosol module, REMO-HAM incorporates many of the updates in physics that are included in recent the ECHAM5-HAM2 version (REMO-HAM has the HAM suffix because it does not have the HAM2 updated tracer structure and the Secondary Organic Aerosol (SOA) module). The main deficiencies of REMO-HAM are the missing SOA module and the online coupling of the HAM module with the radiation scheme (Pietikäinen et al., 2012).

2.2 OH-proxy

The chemistry modules of ECHAM-HAM and REMO-HAM are based on a sulphate aerosol chemistry module described by Feichter et al. (1996). In this module, dimethyl sulfide (DMS), sulfur dioxide (SO_2) and sulphate (SO_4^{2-}) are treated as prognostic variables. For oxidation, the module uses three dimensional monthly mean oxidant fields from hydroxyl (OH), hydrogen peroxide (H_2O_2), ozone (O_3) and nitrogen dioxide (NO_2) (Stier et al., 2005). These fields are calculated/provided by the comprehensive MOZART chemical transport model (Horowitz et al., 2003). Both gas- and aqueous-phase oxidations are included. In the gas phase, SO_2 and DMS are oxidized by OH during the daytime while DMS reacts with the nitrate radical (NO_3) during the night. NO_3 is assumed to be in steady state with its production and loss terms, which both include reactions with NO_2. The reactions of O_3, SO_2 and H_2O_2 are considered in the aqueous phase.

The formation of sulphuric acid (H_2SO_4) occurs via the reaction between the hydroxyl radical OH and sulphur dioxide SO_2; which, in turn, is directly emitted from various anthropogenic and natural sources. SO_2 is also produced in a reaction between DMS

ACPD
14, 8915–8961, 2014

and OH. The OH concentrations are higher during the daytime due to photolysis reactions (source terms) (Seinfeld and Pandis, 1998). As mentioned before, the models use monthly mean fields for OH, which is not a very realistic approach. To overcome this problem, both ECHAM-HAM and REMO-HAM use an artificial diurnal cycle. This is obtained by using the monthly mean values as a baseline and multiplying them with a diurnal coefficient. This coefficient follows a cosine peak between sunrise and sunset and its amplitude is scaled with the day length (thus, the monthly mean values for OH are preserved). Although this approach is more realistic than the original, where the constant values were used, it has some disadvantages: it can overestimate the values for short days, and it is not connected to radiation (for example, below clouds, the concentrations are not affected by the decreased solar radiation).

In order to preserve the speed of the chemical module (keep it as usable as possible for long-term simulations), the calculation method for OH concentrations is replaced with an OH-proxy. Rohrer and Berresheim (2006) presented an equation for approximating OH concentration by using a nonlinear function of the photolysis frequency of ozone $J(O^1D)$ as a predictor. The approach is to build the proxy by using variables that are commonly measured in different sites and can be easily accessed with atmospheric models. Thus, global radiation is used as the main predictor instead of $J(O^1D)$. The reason for this is that global radiation is more commonly available in different datasets and the correlation between these two variables is evident. The construction of the proxy follows a similar approach to that Mikkonen et al. (2011) used for H_2SO_4 concentration. A nonlinear fitting procedure is applied to the measurement data, where the functional form for the proxy is given by

$$[\mathrm{OH}] = a \times \mathrm{Radiation}^b + c, \quad (1)$$

where the exponent b reflects the combined effects of all photolytic processes that generate OH either directly or via production of and recycling from HO_2. The dependence of OH on reactants such as NO_x, hydrocarbons, O_3 or H_2O is condensed into the single pre-exponential coefficient, a. The coefficient c includes all processes that are

ACPD
14, 8915–8961, 2014

light-independent; for example, OH production at nighttime. These coefficients were estimated with OH-measurement data recorded in Hyytiälä, Finland (Petäjä et al., 2009).

The implemented OH-proxy (OH_{proxy}) is:

$$OH_{proxy} = \begin{cases} 3081.0 \cdot \text{Radiation}^{0.8397} & \text{day time} \\ 6.033 \times 10^{4} & \text{night time} \end{cases}, \quad (2)$$

where the units are [molec cm^{-3}] for OH-proxy and [W m^{-2}] for radiation. With this approach, the OH concentrations used by the model are more realistic and are linked to the incoming solar radiation in each grid box on every model level.

2.3 Nucleation scheme

ECHAM-HAM and REMO-HAM use binary sulfuric acid–water nucleation methods by Vehkamäki et al. (2002) and Kazil and Lovejoy (2007), and along with two nucleation schemes for the forested boundary layer: nucleation based on cluster activation (Kulmala et al., 2006) and nucleation based on kinetic activation (Laakso et al., 2004). These empirical schemes are usually employed to calculate the formation rates of 1 (or 1.5) nm clusters. However, the empirical formulas are not based on directly measured cluster formation rates, as the 1 nm rates have been obtained by extrapolation from measured 3 nm particle formation rates (Kerminen and Kulmala, 2002). The extrapolation requires, as input, the cluster growth rate, which often has quite large uncertainty. Furthermore, condensable organics (Kulmala et al., 2013), which are known to participate in cluster growth between 1 and 3 nm, are not included in the current model setup. Taken together, the extrapolation from 3 nm to 1 nm and the modelling of the growth from 1 nm back to 3 nm creates an error in the modelled 3 nm particle formation rates. This unnecessary calculation cycle can be passed as the 3 nm formation rate can be directly parametrized based on observations.

ACPD
14, 8915–8961, 2014

In this work, the formation rate of 3 nm particles J_{3nm} [$cm^{-3} s^{-1}$] is calculated using the kinetic nucleation scheme:

$$J_{3nm} = K \times [H_2SO_4]^2, \quad (3)$$

where $K = 1.417 \times 10^{-15}$ [$cm^3 s^{-1}$] is the kinetic coefficient and $[H_2SO_4]$ is the sulphuric acid concentration in molec cm^{-3}. The value of the kinetic coefficient, K, is based on a comparison of the model results and measurements conducted within this work (not shown).

The default approach of nucleation rate is also modified: kinetic nucleation is not restricted to occur only at the forested boundary layer, but is instead calculated in every grid box. Following the same presumption as in Makkonen et al. (2009), only sulphuric acid is assumed to condense on nucleated particles while they grow to 3 nm in size. There is, however, no nucleation in the cloudy part of the grid boxes, as in this case all the sulphuric acid is removed through condensation. This does not apply for convective clouds, in which only the deposition processes are calculated.

2.4 Simulations

The ECHAM5-HAM data is used at the lateral boundaries of REMO-HAM (Pietikäinen et al., 2012) for aerosol species with an update frequency of 6 h. ERA-Interim data is used to nudge ECHAM5-HAM and as a lateral meteorological boundary forcing for REMO-HAM (Dee et al., 2011). The resolution of T63L31 is applied for ECHAM5-HAM (horizontally 210 km, vertically 31 levels), while for REMO-HAM a resolution of 0.44° (50 km × 50 km) is used with 27 vertical levels. The models have been run for the years 2003–2004 and 2008–2009 with spin-up times of 3 months. The domain for REMO-HAM covers the whole of Europe. To study the nucleation events in more detail, one-hour output resolution for the REMO-HAM simulations is used. For 2003 and 2004, two model versions are used: OH-proxy version including 3 nm nucleation in all grid boxes (henceforth called REMO-OHP), and a normal chemistry version including 3 nm nucleation in all grid boxes (henceforth called REMO-NCH).

ACPD
14, 8915–8961, 2014

Figure 1 shows the orography of the model domain and the measurement sites used in this study. Detailed information about the measurement sites is presented in Table 1.

2.5 Measurement sites and data

Two different approaches for compairing the model results against measurement data are used. Firstly, observation data from three stations, Hyytiälä, Melpitz and San Pietro Capofiume, is used. Details about measurement data and instruments used can be found in Birmili and Wiedensohler (2000); Jaatinen et al. (2009) and Engler et al. (2007). Secondly, literature-based observation data is used to analyse the model results for all 13 stations. The measurement sites, the measurement periods and references to data are presented in Table 1.

2.6 Event classification

The classification of modelled nucleation events is based on two criteria. First, the $J_{3\,\mathrm{nm}}$ values have to be over 0.01 [$\mathrm{cm}^{-3}\,\mathrm{s}^{-1}$] for two sequential hours. This limit comes from the lower detection limit of the instruments used in Hyytiälä and San Pietro Capofiume. Second, for the same time period, the rate of number concentration change with respect to change in logarithmic diameter for 3 nm particles has to be over 2000 $\mathrm{d}N/\mathrm{d}\log_{10} D_p$. This value is derived directly from the aerosol size distributions by comparing the distribution and the $J_{3\,\mathrm{nm}}$ values. According to our tests, this approach classifies the event days realistically. However, some error is introduced in specific cases; for example, if a nucleation event is terminated prematurely due to rain, etc. Nevertheless, these cases are not very common in the model and, based on the testing, these criteria work very well for the modelled data.

The event classification used for measurements (Hyytiälä, Melpitz and San Pietro Capofiume) was conducted by Jaatinen et al. (2009) with the method based on Dal Maso et al. (2005). A day is considered an event day when the formation of new aerosol particles starts at the lowest measurable particle size (diameter 3 nm) and subsequent

ACPD
14, 8915–8961, 2014

growth of the newly formed particles is observed for several hours. The nucleation event classification is based on event clarity; i.e., the number concentrations of the freshly formed particles, and their formation and growth rates. For more details on the classification method, see Hamed et al. (2007).

3 Comparison with measurements

3.1 J_{3nm} values

The measured and modelled J_{3nm} values are compared in Fig. 2. Since the measurement data is only for the nucleation event days, the same approach is made to model data using the event classification method described in Sect. 2.6.

The mean J_{3nm} rates show that REMO-OHP is able to reproduce measured values at Hyytiälä, although overall there is some underestimation (the relative change of 2-year mean $\Delta_r = -71\,\%$). The highest measured rates are not captured during the spring, but the summer values are well reproduced. For REMO-NCH, the values are also quite realistic, but overestimated ($\Delta_r = 66\,\%$). The same behaviour can also be seen at Melpitz and San Pietro Capofiume. At these locations, the overestimation of REMO-NCH is larger, especially at San Pietro Capofiume ($\Delta_r = -35\,\%$ for REMO-OHP and $\Delta_r = 590\,\%$ for REMO-NCH at Melpitz, and $\Delta_r = -60\,\%$ for REMO-OHP and $\Delta_r = 393\,\%$ for REMO-NCH at San Pietro Capofiume). Based on these results, REMO-OHP is able to more realistically reproduce the J_{3nm} values than REMO-NCH. The length of the events is also an important factor for the total number of nucleated particles. This is analysed in the next section.

3.2 Start and end time/duration of events

The measurement data for Hyytiälä, Melpitz and San Pietro Capofiume also includes the nucleation event start time, end time and (calculated) length. For these variables, monthly statistics for the measurements and modelled results are derived.

ACPD
14, 8915–8961, 2014

Figure 3 shows that, at Hyytiälä, the REMO-OHP results for the event's start time are in good agreement with the measurements. REMO-OHP had some problems during the spring and summer of 2003, but otherwise the simulated nucleation events do not differ significantly from the measurements. On the other hand, the REMO-NCH events started 1–3 h too early. The difference is biggest during the summer months, especially during 2004. The end times of the events show more fluctuations, but overall the agreement between the measurements and REMO-OHP is good. The only problematic time period is the summer/autumn of 2004. During this time, REMO-OHP shows a strong delay in event end times (up to 5 h). Similar behaviour can be seen in the REMO-NCH results, which tend to delay the event ends for almost the whole modelled period. This naturally means that the event lengths are overestimated with REMO-NCH. REMO-OHP can reproduce the event length realistically for most of the modelled period, excluding the problematic summer/autumn of 2004.

At Melpitz, REMO-OHP can catch the event start times very well for 2003. During 2004, the model gives too-early start times for the first half of the year while, for the second half, the start times are delayed. The difference stays within a couple of hours. In REMO-NCH, the events start a few hours too early. The difference is highest during the summer and almost disappears during the winter (no data, unfortunately). The end time of the events at Melpitz is not very well captured by either of the models, which show much later end times than the measurements. In particular, the REMO-NCH model has a tendency to have too-long nucleation, which is seen clearly in the event length. The overestimation is very high (10 h) during the summer times and decreases in the winter (2 h). REMO-OHP shows a similar trend, but the values are much lower (4 h during the summer and 2 during the winter).

The aerosol distributions were also compared with the measurements analysed by Hamed et al. (2010) (not shown). This comparison showed that the model results underestimate the number concentration of particles > 100 nm by a factor of two (similar behaviour can be also seen for the aerosol distributions in an earlier study by Pietikäinen et al., 2012). One possible reason for this is the missing SOA growth, which would

ACPD
14, 8915–8961, 2014

lead to higher concentrations of particles > 100 nm. Either way, the lower particle numbers lead to lower surface area and condensation sink. This might be the key factor in understanding why the model overestimates the event lengths in Fig. 3 at Melpitz: if the condensation of H_2SO_4 is too low during the nucleation and especially after, the remaining H_2SO_4 will continue to cause nucleation until it has been removed.

The results from San Pietro Capofiume show that REMO-OHP gives almost identical event start times for 2003 when compared to the measurements. During the beginning of 2004, REMO-OHP started nucleation slightly too early, but caught up with the start times again during the summer. REMO-NCH systematically started the events too early. Once again, the difference is smallest during the winter and highest during the summer. The event end times are delayed with both models, which influences the event lengths. REMO-OHP overestimates the event lengths by 2 h, whereas REMO-NCH overestimates by 2–10 h (maximum being in the summer). The same mechanism applies here as for Melpitz: the lower condensation sink of H_2SO_4 in the model causes the delays in the nucleation end time (increased lengths).

3.3 Fraction of event days

The fraction of event days per month is analyzed from all measurement stations. This subsection is divided into two parts, which are based on the simulation periods.

3.3.1 Years 2003 and 2004

The measured and modelled monthly fractions of nucleation days for Hyytiälä, Melpitz and San Pietro Capofiume are shown in Fig. 4. The measurement data has some gaps, because measurements were not available for the entire two-year period (details in Table 1).

REMO-OHP underestimates the fraction of nucleation days per month in spring and overestimates it in early summer at Hyytiälä. For autumn, the model underestimates the fraction in 2003 (reproducing only half of the nucleation days), but captures the

ACPD
14, 8915–8961, 2014

events in 2004. REMO-NCH overestimates the fraction almost throughout the modelling period, going up to five times higher event frequency. Late autumn in 2003 and spring 2004 are the only times when REMO-NCH is underestimating or being even close with the measurements. Overall, the values from the model simulations are not a perfect match, but REMO-OHP is showing much better agreement.

For Melpitz, Fig. 4 shows that REMO-OHP slightly overestimated the nucleation events for the year 2003 (0–15 %). For 2004, REMO-OHP overestimated the values for the first half of the year (up to five times) and underestimated for the second; for example, getting less than half of the events during September. With REMO-NCH, the fraction of monthly nucleation days is overestimated in every month. The low fraction in measurements for summer 2004 can be partly explained by the high number of undefined days (up to 14 days per month) (Jaatinen et al., 2009).

At San Pietro Capofiume, REMO-OHP tends to predict nucleation events too frequently by 30–50 % for both years, especially during wintertime (Fig. 4). If January and February are disregarded, the pattern of the first year is well captured by REMO-OHP. REMO-NCH shows high overestimations, especially during summertime. For many months, REMO-NCH show nucleation fractions of 1.0. Even during the winter, more than 60 % of the days show nucleation events. Pietikäinen et al. (2012) showed that the model has a positive SO_2 bias, which can lead to elevated H_2SO_4 values. The bias is relatively high in polluted areas, and location such as San Pietro Capofiume falls into this category (Laaksonen et al., 2005, and references therein). Despite the improved OH chemistry presented in this work, the results for SPC are affected by the positive SO_2 bias.

In addition to the measurement-based analysis conducted for Hyytiälä, Melpitz and San Pietro Capofiume, an analysis based on observation data from literature is performed. Figure 5 shows the fraction of nucleation days per month for these locations (more details in Table 1). For Mace Head, data from Yoon et al. (2006) are used. Two types of nucleation events are observed in Mace Head: the coastal events, driven by iodine species emitted by algae during low tides, and the continental type of events; i.e.,

ACPD
14, 8915–8961, 2014

sulphuric acid-driven events similar to those observed at the other stations. The former type of nucleation is not included in REMO-HAM, making the comparison between simulations and observations somewhat complicated. However, Yoon et al. (2006) provided two kinds of nucleation event statistics: the total number of events, and the number of events for cases in which clean marine air masses advected over tidal areas to the measurement station. While some of the latter events may be of the continental type, it is clear that most of them are coastal (see also O'Dowd et al., 2002). Similarly, it is likely that the majority of the rest of the events (polluted cases i.e., total events minus clean events) are of the continental type.

Figure 5 shows the total number of nucleation events and the difference between the total and clean air mass cases (shown as ΔYoon et al., 2006). The model results for Mace Head show that, if compared to all event cases, REMO-OHP underestimates the nucleation days for the whole simulation period. On the other hand, REMO-NCH gives reasonably realistic results. In addition, the overestimation seen before in REMO-NCH is not present. However, if the ΔYoon et al. (2006) results are compared, results from REMO-OHP show better agreement. The model still underestimates the event numbers during both winter and spring 2003, but the absolute difference is much smaller. During spring 2004, and both summers and autumns, REMO-OHP is able to capture the measured statistics that have even slight overestimations in some cases. REMO-NCH overestimates the values for all months.

At Hohenpeißenberg, REMO-OHP reproduces the measured values with good accuracy. Also, the yearly cycle is somewhat similar with measurements. There are some months; for example during spring, when the model overestimates the number of event days. On the other hand, underestimation occurs in autumn and winter, but the absolute difference is quite small. REMO-NCH shows realistic results only during the winter time. During other periods, the model overestimates the event day fraction 3–5 times.

The results from Värriö show that REMO-OHP is underestimating the measured nucleation event frequencies by roughly a factor of two. The biggest difference is the almost totally missing autumn nucleation. This is more realistically captured with REMO-

ACPD
14, 8915–8961, 2014

NCH, which overestimates the values for the first half of the year, but is close with measurements otherwise. Similarly, the missing autumn nucleation in REMO-OHP can be seen at Pallas. There, REMO-OHP does not underestimate the values as much as at Värriö. Besides autumn, only the spring of 2003 is underestimated; otherwise, values are close to measurements. REMO-NCH has similar behaviour at Pallas as at Värriö, although the overestimation is slightly more frequent.

Autumn nucleation events also seem to be a problem for REMO-OHP at Vavihill. In addition, the winter nucleation is underestimated or missing, but otherwise the model is able to reproduce the event fractions realistically. REMO-NCH is able to get the late-winter events, but overestimates the summer values. Moreover, the autumn is better captured with REMO-NCH than REMO-OHP.

It is not clear why the autumn nucleation is missing from the simulated climate. In order to rule out problems in the nucleation classification method, the banana plots showing the evolution of aerosol size distribution during the day were studied (details not shown here). The banana plots did not show any clear nucleation events during autumn, which means that the classification does work. There are few candidates to explain why the autumn time nucleation is not captured by the model. It is possible that the sulphuric acid concentrations are too low. This is supported by the earlier study on black carbon concentration over Finland by Hienola et al. (2013), who reported deficiencies in the used emission database. Although the analysis in their study was done for black carbon, the database can also have similar problems for other species, such as SO_2. A higher resolution (spatial and time-wise) database could help to improve the sulphuric acid concentrations, especially at remote places like Värriö and Pallas, where small concentration changes could have big impact on nucleation. On the other hand, the nucleation scheme used can, itself, be too simple. Taking into account other volatile compounds could improve the results (Andreae, 2013). Also, the used kinetic coefficient should ideally not be treated as a constant, as the nucleation rates probably vary with meteorological parameters and some chemical species. However, the current

ACPD
14, 8915–8961, 2014

level of understanding of the nucleation process does not permit accounting for these factors.

3.3.2 Years 2008 and 2009

For 2008 and 2009 the simulations are conducted only with REMO-OHP. As the previous sections have shown, REMO-NCH produces too-high nucleation rates and event frequencies. For this reason, in Fig. 6, only the REMO-OHP model run is shown.

At Hyytiälä, REMO-OHP shows that the predicted nucleation events in springtime are underestimated, during summer some overestimation can be seen and in autumn the nucleation seems to be missing. Nevertheless, the yearly cycle is captured (autumn excluded) and the values are reasonably close to the measurements. In Melpitz, the model underestimates the fraction of events, while the analysis for 2003 and 2004 showed overestimations (Fig. 4). The underestimation is fairly strong for both years. The yearly cycle is captured, although the winter events are missing. The emission database used is for the year 2000 (Dentener et al., 2006), and it is surprising that the model is underestimating the 2008 and 2009 result, because the SO_2 emissiona are known to have decreases over the last 2–3 decades (Hamed et al., 2010, and references therein). On the other hand, this could implicate the same reason that was speculated in the previous section: the nucleation scheme used needs to have more input parameters in terms of other compounds.

For San Pietro Capofiume, the data coverage from literature is quite limited. Still, the same features as for 2003 and 2004 can be seen: the model overestimates the number of nucleation events. At Mace Head, the results show similar underestimation as in 2003 and 2004. The results from REMO-OHP at Hohenpeißenberg for 2003 and 2004 were very close to measurements. For 2008 and 2009, the model does not capture all the events. Again, taking into account the emission reductions for sulphuric species, this result is surprising. It appears that, although sulphuric acid can be considered the main driver for nucleation, the simplistic approach using it as the only participating species should be improved. The same applies to Pallas, where similar

ACPD
14, 8915–8961, 2014

underestimation can be seen. At Vavihill, the model can reproduce the measured values better, although it has a slightly underestimating bias.

The Finokalia results show large overestimations in spring, summer and autumn. In winter, the model tends to underestimate the results when compared to both literature sources. The reason for the overestimation could stem from too-high solar radiation levels in the model. The model cloudiness was, therefore, compared against ERA-Interim data, but no clear bias was found. Another possible reason could be the DMS and OH concentrations. As mentioned in Sect. 2.2, DMS is oxidized by OH during the daytime. The location of Finokalia provides enough sunlight for OH; so, if these two are overestimated, the nucleation will show patterns similar to Fig. 6. The influence of other sulphuric acid sources cannot be excluded; but, taking the Finokalia location into account, the combination of overestimated DMS and OH appears to be the most credible explanation. Also, the proxy is quite simple and the results from Finokalia show that more input parameters should be employed in order to get a better representation of the regional characteristics.

At Cabauw, the model predicts a yearly nucleation maximum during the spring; whereas, in measurements, it is in the summer. The modelled values are slightly lower than the measured, and the autumn peaks are missing. At K-Puszta, the values are closer to the measurements. For the summer, the nucleation event frequency is even overestimated. The yearly maximum is modelled more towards the summer. The measurements show that it should be during the springtime. Overall, the values are quite realistic and of the same magnitude as the measurements.

Puy de Dôme is a location where the model is giving very realistic results. The overall tendency is slightly underestimated, but the yearly cycle is well captured. This also holds true for Jungfraujoch, although there the model has some overestimation. Overall, these results are very good considering the mountainous location, which are known to be difficult for the model dynamics (Pietikäinen et al., 2012).

ACPD
14, 8915–8961, 2014

3.4 Vertical extent of nucleation

Figure 7 shows example periods of modelled nucleation at Hyytiälä, Melpitz and San Pietro Capofiume. The nucleation events are strong at Hyytiälä, but the growth seems to be missing. There are at least two possible explanations for this: the model lacks condensable organics, and the representation of the aerosol population with 7 log-normal modes leads to problems, as is shown by Korhola et al. (2013). In the latter case, the particles grow due to the condensation of sulphuric acid and coagulation, but the mode structure is unable to show this as a continuous phenomena. Instead, Fig. 7 shows how the particles have "moved" directly to Aitken/accumulation mode sizes.

The vertical evolution of events reveals that, at Hyytiälä, nucleation takes place mostly inside the boundary layer. In some cases, the concentrations above the boundary layer are also very high. This is a known phenomena in ECHAM5-HAM (Kazil et al., 2010) and has also been shown to exist REMO-HAM (Pietikäinen et al., 2012). In addition, the OH proxy is a function of radiation and is based on surface measurements. This might cause some error at higher altitudes.

At Melpitz, the nucleation bursts are much stronger than at Hyytiälä (Fig. 7). Noticeable is that, during the nighttime the accumulation mode number concentration is increasing. This happens when the particles in Aitken mode coagulate with the accumulation mode particles. As mentioned before, the model does not have an online SOA module, which means that the only condensing species is sulphuric acid. During the night, the H_2SO_4 concentrations are low, so only the coagulation is active. As there are not many coarse-mode particles, the accumulation mode does not have bigger particles to coagulate and the number concentration starts to increase. Like at Hyytiälä (although shown much more clearly), the Aitken/accumulation mode is flushed away during the morning. This can be also seen from measurements (not shown here). The reason for this is the boundary layer mixing during the morning, which is caused by solar heating. At the same time, nucleation bursts can be seen. Vertically the situation is similar to that at Hyytiälä: in some cases, nucleation bursts exceed the boundary

ACPD
14, 8915–8961, 2014

layer. There are also some high number concentrations well above the boundary layer height. It also seems that, in some downdrafts, the particles concentrations are high. This could be explained with earlier formed convective clouds: the vertical transport moves SO_2 and H_2SO_4 to the mid and upper troposphere. There, the gases have the potential to trigger nucleation; and, eventually, the particles will to come down (Kazil et al., 2006). In the model, all the gas-phase sulphate is assumed to condense to cloud droplets in stratiform clouds, but not in convective clouds. The wet deposition is calculated in and below convective clouds, but during the vertical transport no gas-phase sulphate is assumed to condense to cloud droplets. This, and the evaporation of clouds, means that the convective clouds act as an elevator for the aerosol species.

Laaksonen et al. (2005) reported that, at San Pietro Capofiume, the nucleated particles grow to 100 nm size in 10 h (on average, measurements from 24 March 2002 to 24 August 2004). This fits quite reasonably to our results (Fig. 7). Laaksonen et al. (2005) also showed that the largest particles reach sizes larger than 200 nm by midnight. The model also seems to be able to reproduce this behaviour. During 12–13 February 2004, the influence of precipitation can be seen: almost all of the particles are flushed from the boundary layer.

3.5 Spatial extent of events

One interesting aspect of climate models is that the spatial extent of nucleation events can be studied. The approach used here is to apply the classification method explained in Sect. 3.3 for all grid boxes in every output step (1 h) and average only these cases.

Figure 8 shows the simulated average (when event classification criteria is met) nucleation rates $J_{3\,nm}$. Nucleation occurs in the model throughout Europe, with "hot spots" of strong nucleation near the peak emissions sources (industrial areas, cities, etc.). Also, the ship tracks can be seen from the averaged nucleation values. More locally; for example, at Melpitz, the high nucleation rates seem to be linked to big industrial-point SO_2 sources (power generation) in the easternmost parts of Germany and neighbouring countries (Czech Republic, Poland). This shows that the nucleation events in the

ACPD
14, 8915–8961, 2014

model can go from very local scales to hundreds of kilometers and is in good agreement with previous studies of the spatial extent of nucleation (for example, over North America by Crippa and Pryor, 2013).

In order to calculate the strongest nucleation events in Europe, J_{3nm} is averaged for all output steps. Figure 9 shows the seasonal mean values for 2003 and 2004 (results are almost identical for 2008 and 2009 and are, thus, not shown). The nucleation is strongest during the spring and summer, as expected. Again, the strong emission sources, as well as ship tracks, can be clearly seen from the maps. During autumn, nucleation rates are low in Fennoscandia, as was also seen in the nucleation event frequency statistics in Sect. 3.3, and could be explained by cloud cover, precipitation, emissions, constant kinetic nucleation and OH-proxy coefficients, etc. The missing autumn nucleation for Fennoscandia can be a mixture of these elements.

Nucleation events are naturally influenced by meteorological variables. This leads to very different nucleation events on a spatial scale. Figure 10 shows six nucleation event snapshots taken from the years 2008 and 2009. The top left figure (3 March 2008 12:00 UTC) shows how most parts of Europe are without considerable NPF rates, whereas Northern Africa has quite strong events. The top centre figure (16 June 2008 11:00 UTC) shows nucleation happening mostly near eastern part of Mediterranean Sea. The top right (24 December 2008 10:00 UTC) is an example of weak nucleation. The lower left (1 February 2009 10:00 UTC) shows strong nucleation events over Ukraine and Western Russia, whereas Western Europe is without events. Almost the opposite is seen in the lower centre (21 April 2009 12:00 UTC) figure, where Eastern Europe is without nucleation, but Western and Central Europe are experiencing a strong nucleation event. The last figure on the lower right (16 September 2009 12:00 UTC) show a situation where Central Europe is without nucleation, but Western and Eastern Europe are having events.

ACPD
14, 8915–8961, 2014

3.6 Boundary layer analysis

Using the information of the mean nucleation event length, the number of nucleation days per year and the mean formation rate from Hamed et al. (2007), combined with the height information of a well-mixed boundary layer from Laaksonen et al. (2005), a rough estimate of the yearly number of nucleated 3 nm particles in the boundary layer over San Pietro Capofiume can be calculated: $3.6 \times 10^{15}\,\#\,m^{-2}$. The equivalent value can be calculated from the model output for the grid box where San Pietro Capofiume is located without any estimations. The results are in Table 2, where the values for San Pietro Capofiume and Europe (only land points) are shown.

The values for San Pietro Capofiume are lower than the literature estimate. However, the difference is less than a factor of two. Both the model and the literature estimates, especially the latter, have a number of possible (unquantified) error sources; therefore, such a difference appears quite reasonable.

The monthly production of 3 nm particles in the European boundary layer is shown in Fig. 11. The production has a minimum during the winter and a maximum during the summer. This shows that, overall, the simulated annual cycle of nucleation in the European boundary layer is more similar to that observed in San Pietro Capofiume (summer maximum, winter minimum Hamed et al., 2007) than the cycle in Hyytiälä (spring and autumn maxima Kulmala et al., 2004).

4 Conclusions

A measurement-based OH proxy was implemented in the regional aerosol-climate model REMO-HAM. This supersedes a former version that used monthly mean fields for OH with an artificial diurnal cycle. The new implemented proxy is a function of radiation, thus linking the cloudiness of the model to the OH concentrations. In addition, the nucleation rate expression was changed to directly calculate the 3 nm particles (in diameter).

ACPD
14, 8915–8961, 2014

Despite some underestimation in different regions, the new model version gives more realistic nucleation rates for 3 nm particles compared to the original model version, which overestimated the observed nucleation rates. Overall, the agreement with observations has been considerably improved.

Nucleation event statistics were analysed at 13 different European sites. The results show good agreement at some sites, but for some the yearly cycle was not captured. Also, for many (northern) sites, the OH-proxy model fails to predict nucleation events during autumn, whereas they are frequently observed. A more detailed analysis was done for three measurement sites (Hyytiälä, Melpitz and San Pietro Capofiume). The results show that the monthly means for start time, end time and length of nucleation events are quite well captured. The main problem is that the nucleation in the model tends to continue longer than in observations. The main reason for this can be the missing organic growth of particles, which leads to lower number concentration of particles > 100 nm. This decreases the condensation sink of sulphuric acid and the remaining sulphuric acid will keep the nucleation active for longer period of time.

The vertical extension of nucleation events was also analysed. As expected, the events mainly happen inside the boundary layer. Because of the simple form of the proxy, the model simulates nucleation also in the upper troposphere. On the other hand, this feature has been reported also in earlier versions and in the global model ECHAM-HAM (Kazil et al., 2010; Pietikäinen et al., 2012). The distribution plots show that nucleation bursts are realistically captured, but the growth to larger particles is not as continuous as in measurements due to the missing organic condensation and the structure of the modal aerosol model (Korhola et al., 2013).

The spatial distribution of nucleation events showed that strongest events occur close to the major sources of sulphur dioxide. It is worth to note that large point sources of SO_2, such as in adjacent East European countries, seem to contribute to the strong nucleation events happening at Melpitz. Seasonally, the trend over Europe is to have strong nucleation during the summer and less during the winter. The same was shown when the total nucleation was calculated in the European boundary layer.

ACPD
14, 8915–8961, 2014

Small changes in the simple chemistry module can lead to big improvements in results, as is shown in this study. In addition, using a proxy does not increase the computational burden of the model at all. This makes the approach very useful in aerosol-climate models. To improve the system, more work should be targeted to connect the coefficients used in the proxy with regional features. This could mean, for example, two-dimensional maps for the coefficients. Also, taking into account the seasonal effects, the proxy could provide even more realistic results; this will be studied in a subsequent analysis. The same applies also for the nucleation coefficient (activation/kinetic). The regional features; for example, NPF and its realistic connection to the surrounding climate, does play an important role for European and global nucleation events.

Acknowledgements. This work was supported by the Academy of Finland (Research Programme for Climate Change FICCA, project 140748, and the Center of Excellence Programme, project 1118615), by the strategic funding of the University of Eastern Finland, and by the EU FP7 IP PEGASOS (FP7-ENV-2010/265148). The authors would like to thank T. Nieminen for providing the Hyytiälä event classification data.

References

Andreae, M. O.: The aerosol nucleation puzzle, Science, 339, 6122, 911–912, doi:10.1126/science.1233798, 2013. 8931

Birmili, W. and Wiedensohler, A.: New particle formation in the continental boundary layer: meteorological and gas phase parameter influence, Geophys. Res. Lett., 27, 3325–3328, 2000. 8925, 8949

Birmili, W., Berresheim, H., Plass-Dülmer, C., Elste, T., Gilge, S., Wiedensohler, A., and Uhrner, U.: The Hohenpeissenberg aerosol formation experiment (HAFEX): a long-term study including size-resolved aerosol, H_2SO_4, OH, and monoterpenes measurements, Atmos. Chem. Phys., 3, 361–376, doi:10.5194/acp-3-361-2003, 2003. 8949

Boulon, J., Sellegri, K., Venzac, H., Picard, D., Weingartner, E., Wehrle, G., Collaud Coen, M., Bütikofer, R., Flückiger, E., Baltensperger, U., and Laj, P.: New particle formation and ultrafine charged aerosol climatology at a high altitude site in the Alps (Jungfraujoch, 3580 m a.s.l.,

ACPD
14, 8915–8961, 2014

Switzerland), Atmos. Chem. Phys., 10, 9333–9349, doi:10.5194/acp-10-9333-2010, 2010. 8949

Boulon, J., Sellegri, K., Hervo, M., Picard, D., Pichon, J.-M., Fréville, P., and Laj, P.: Investigation of nucleation events vertical extent: a long term study at two different altitude sites, Atmos. Chem. Phys., 11, 5625–5639, doi:10.5194/acp-11-5625-2011, 2011. 8949

Crippa, P. and Pryor, S. C.: Spatial and temporal scales of new particle formation events in eastern North America, Atmos. Environ., 75, 257–264, 2013. 8936

Dal Maso, M., Kulmala, M., Riipinen, I., Wagner, R., Hussein, T., Aalto, P., and Lehtinen, K. E. J.: Formation and growth of fresh atmospheric aerosols: eigth years of aerosol size distribution data from SMEAR II, Hyytiälä, Finland, Boreal Environ. Res., 10, 323–336, 2005. 8925

Dal Maso, M., Sogacheva, L., Aalto, P. P., Riipinen, I., Komppula, M., Tunved, P., Korhonen, L., Suur-uski, V., Hirsikko, A., Kurtén, T., Kerminen, V.-M., Lihavainen, H., Viisanen, Y., Hansson, H.-C., and Kulmala, M.: Aerosol size distribution measurements at four Nordic field stations: identification, analysis and trajectory analysis of new particle formation bursts, Tellus B, 59, 350–361, 2007. 8949

Dee, D. P., Uppala, S. M., Simmons, A. J., Berrisford, P., Poli, P., Kobayashi, S., Andrae, U., Balmaseda, M. A., Balsamo, G., Bauer, P., Bechtold, P., Beljaars, A. C. M., van de Berg, L., Bidlot, J., Bormann, N., Delsol, C., Dragani, R., Fuentes, M., Geer, A. J., Haimberger, L., Healy, S. B., Hersbach, H., Hólm, E. V., Isaksen, L., Kållberg, P., Köhler, M., Matricardi, M., McNally, A. P., Monge-Sanz, B. M., Morcrette, J.-J., Park, B.-K., Peubey, C., de Rosnay, P., Tavolato, C., Thépaut, J.-N., and Vitart, F.: The ERA-Interim reanalysis: configuration and performance of the data assimilation system, Q. J. Roy. Meteor. Soc., 137, 553–597, doi:10.1002/qj.828, 2011. 8924

Dentener, F., Kinne, S., Bond, T., Boucher, O., Cofala, J., Generoso, S., Ginoux, P., Gong, S., Hoelzemann, J. J., Ito, A., Marelli, L., Penner, J. E., Putaud, J.-P., Textor, C., Schulz, M., van der Werf, G. R., and Wilson, J.: Emissions of primary aerosol and precursor gases in the years 2000 and 1750 prescribed data-sets for AeroCom, Atmos. Chem. Phys., 6, 4321–4344, doi:10.5194/acp-6-4321-2006, 2006. 8932

Engler, C., Rose, D., Wehner, B., Wiedensohler, A., Brüggemann, E., Gnauk, T., Spindler, G., Tuch, T., and Birmili, W.: Size distributions of non-volatile particle residuals (D_p < 800 nm) at a rural site in Germany and relation to air mass origin, Atmos. Chem. Phys., 7, 5785–5802, doi:10.5194/acp-7-5785-2007, 2007. 8925, 8949

ACPD
14, 8915–8961, 2014

Feichter, J., Kjellström, E., Rodhe, H., Dentener, F., Lelieveld, J., and Roelofs, G.-J.: Simulation of the tropospheric sulfur cycle in a global climate model, Atmos. Environ., 30, 1693–1707, 1996. 8921

Fountoukis, C., Riipinen, I., Denier van der Gon, H. A. C., Charalampidis, P. E., Pilinis, C., Wiedensohler, A., O'Dowd, C., Putaud, J. P., Moerman, M., and Pandis, S. N.: Simulating ultrafine particle formation in Europe using a regional CTM: contribution of primary emissions versus secondary formation to aerosol number concentrations, Atmos. Chem. Phys., 12, 8663–8677, doi:10.5194/acp-12-8663-2012, 2012. 8919

Hagemann, S.: An improved land surface parameter data set for global and regional climate models, MPI Report No. 336, Max Planck Institute for Meteorology, Hamburg, 28 pp., 2002. 8921

Hamed, A., Joutsensaari, J., Mikkonen, S., Sogacheva, L., Dal Maso, M., Kulmala, M., Cavalli, F., Fuzzi, S., Facchini, M. C., Decesari, S., Mircea, M., Lehtinen, K. E. J., and Laaksonen, A.: Nucleation and growth of new particles in Po Valley, Italy, Atmos. Chem. Phys., 7, 355–376, doi:10.5194/acp-7-355-2007, 2007. 8926, 8937

Hamed, A., Birmili, W., Joutsensaari, J., Mikkonen, S., Asmi, A., Wehner, B., Spindler, G., Jaatinen, A., Wiedensohler, A., Korhonen, H., Lehtinen, K. E. J., and Laaksonen, A.: Changes in the production rate of secondary aerosol particles in Central Europe in view of decreasing SO_2 emissions between 1996 and 2006, Atmos. Chem. Phys., 10, 1071–1091, doi:10.5194/acp-10-1071-2010, 2010. 8927, 8932

Hari, P. and Kulmala, M.: Station for Measuring Ecosystem–Atmosphere Relations (SMEAR II), Boreal Environ. Res., 10, 315–322, 2005. 8949

Hienola, A. I., Pietikäinen, J.-P., Jacob, D., Pozdun, R., Petäjä, T., Hyvärinen, A.-P., Sogacheva, L., Kerminen, V.-M., Kulmala, M., and Laaksonen, A.: Black carbon concentration and deposition estimations in Finland by the regional aerosol–climate model REMO-HAM, Atmos. Chem. Phys., 13, 4033–4055, doi:10.5194/acp-13-4033-2013, 2013. 8931

Horowitz, L. W., Walters, S., Mauzerall, D. L., Emmons, L. K., Rasch, P. J., Granier, C., Tie, X., Lamarque, J.-F., Schultz, M. G., Tyndall, G. S., Orlando, J. J., and Brasseur, G. P.: A global simulation of tropospheric ozone and related tracers: description and evaluation of MOZART, version 2, J. Geophys. Res., 108, 4784, doi:10.1029/2002JD002853, 853, 2003. 8921

Jaatinen, A., Hamed, A., Joutsensaari, J., Mikkonen, S., Birmili, W., Wehner, B., Spindler, G., Wiedensohler, A., Decesari, S., Mircea, M., Facchini, M. C., Junninen, H., Kulmala, M., Lehtinen, K. E. J., and Laaksonen, A.: A comparison of new particle formation events in the

ACPD
14, 8915–8961, 2014

boundary layer at three different sites in Europe, Boreal Environ. Res., 14, 481–498, 2009. 8925, 8929, 8949

Jacob, D.: A note to the simulation of the annual and inter-annual variability of the water budget over the Baltic Sea drainage basin, Meteorol. Atmos. Phys., 77, 61–73, 2001. 8921

Jacob, D. and Podzun, R.: Sensitivity studies with the regional climate model REMO, Meteorol. Atmos. Phys., 63, 119–129, 1996. 8921

Jung, J., Fountoukis, C., Adams, P. J., and and Pandis, S. N.: Simulation of in situ ultrafine particle formation in the eastern United States using PMCAMx-UF, J. Geophys. Res., 15, 03203, doi:10.1029/2009JD012313, 2010. 8919

Kazil, J. and Lovejoy, E. R.: A semi-analytical method for calculating rates of new sulfate aerosol formation from the gas phase, Atmos. Chem. Phys., 7, 3447–3459, doi:10.5194/acp-7-3447-2007, 2007. 8918, 8923

Kazil, J., Lovejoy, E. R., Barth, M. C., and O'Brien, K.: Aerosol nucleation over oceans and the role of galactic cosmic rays, Atmos. Chem. Phys., 6, 4905–4924, doi:10.5194/acp-6-4905-2006, 2006. 8935

Kazil, J., Stier, P., Zhang, K., Quaas, J., Kinne, S., O'Donnell, D., Rast, S., Esch, M., Ferrachat, S., Lohmann, U., and Feichter, J.: Aerosol nucleation and its role for clouds and Earth's radiative forcing in the aerosol-climate model ECHAM5-HAM, Atmos. Chem. Phys., 10, 10733–10752, doi:10.5194/acp-10-10733-2010, 2010. 8918, 8934, 8938

Kerminen, V.-M. and Kulmala, M.: Analytical formulae connecting the "real" and the "apparent" nucleation rate and the nuclei number concentration for atmospheric nucleation events, J. Aerosol Sci., 33, 609–622, 2002. 8923

Kerminen, V.-M., Lihavainen, H., Komppula, M., Viisanen, Y., and Kulmala, M.: Direct observational evidence linking atmospheric aerosol formation and cloud droplet activation, Geophys. Res. Lett., 32, L14803, doi:10.1029/2005GL023130, 2005. 8917

Kokkola, H., Hommel, R., Kazil, J., Niemeier, U., Partanen, A.-I., Feichter, J., and Timmreck, C.: Aerosol microphysics modules in the framework of the ECHAM5 climate model – intercomparison under stratospheric conditions, Geosci. Model Dev., 2, 97–112, doi:10.5194/gmd-2-97-2009, 2009.

Korhola, T., Kokkola, H., Korhonen, H., Partanen, A.-I., Laaksonen, A., Lehtinen, K. E. J., and Romakkaniemi, S.: Reallocation in modal aerosol models: impacts on predicting aerosol radiative effects, Geosci. Model Dev., 7, 161–174, doi:10.5194/gmd-7-161-2014, 2014. 8934, 8938

ACPD
14, 8915–8961, 2014

Kotlarski, S.: A Subgrid Glacier Parameterisation for Use in Regional Climate Modelling, Ph.D. thesis, University of Hamburg, Max Planck Institute for Meteorology, Reports on Earth System Science, No. 42, 2007. 8921

Kristensson, A., Dal Maso, M., Swietlicki, E., Hussein, T., Zhou, J., Kerminen, V., and Kulmala, M.: Characterization of new particle formation events at a background site in Southern Sweden: relation to air mass history, Tellus B, 60, doi:10.3402/tellusb.v60i3.16927, 2011. 8949

Kuang, C., McMurry, P. H., McCormick, A. V., and Eisele, F. L.: Dependence of nucleation rates on sulfuric acid vapor concentration in diverse atmospheric locations, J. Geophys. Res., 113, 10209, doi:10.1029/2007JD009253, 2008. 8918

Kulmala, M., Vehkamäki, H., Petäjä, T., Dal Maso, M., Lauri, A., Kerminen, V.-M., Birmili, W., and McMurry, P. H.: Formation and growth rates of ultrafine atmospheric particles: a review of observations, J. Aerosol Sci., 35, 143–176, 2004. 8917, 8937

Kulmala, M., Lehtinen, K. E. J., and Laaksonen, A.: Cluster activation theory as an explanation of the linear dependence between formation rate of 3nm particles and sulphuric acid concentration, Atmos. Chem. Phys., 6, 787–793, doi:10.5194/acp-6-787-2006, 2006. 8918, 8923

Kulmala, M., Kontkanen, J., Junninen, H., Lehtipalo, K., Manninen, H. E., Nieminen, T., Petäjä, T., Sipilä, M., Schobesberger, S., Rantala, P., Franchin, A., Jokinen, T., Järvinen, E., Äijälä, M., Kangasluoma, J., Hakala, J., Aalto, P. P., Paasonen, P., Mikkilä, J., Vanhanen, J., Aalto, J., Hakola, H., Makkonen, U., Ruuskanen, T., Mauldin, R. L., Duplissy, J., Vehkamäki, H., Bäck, J., Kortelainen, A., Riipinen, I., Kurtén, T., Johnston, M. V. Smith, J. N., Ehn, M., Mentel, T. F., Lehtinen, K. E. J., Laaksonen, A., Keminen, V.-M., and Worsnop, D.: Direct observations of atmospheric aerosol nucleation, Science, 22, 911–912, 2013. 8923

Laakso, L., Anttila, T., Lehtinen, K. E. J., Aalto, P. P., Kulmala, M., Hõrrak, U., Paatero, J., Hanke, M., and Arnold, F.: Kinetic nucleation and ions in boreal forest particle formation events, Atmos. Chem. Phys., 4, 2353–2366, doi:10.5194/acp-4-2353-2004, 2004. 8918, 8923

Laakso, L., Merikanto, J., Vakkari, V., Laakso, H., Kulmala, M., Molefe, M., Kgabi, N., Mabaso, D., Carslaw, K. S., Spracklen, D. V., Lee, L. A., Reddington, C. L., and Kerminen, V.-M.: Boundary layer nucleation as a source of new CCN in savannah environment, Atmos. Chem. Phys., 13, 1957–1972, doi:10.5194/acp-13-1957-2013, 2013. 8919

ACPD
14, 8915–8961, 2014

Laaksonen, A., Hamed, A., Joutsensaari, J., Hiltunen, L., Cavalli, F., Junkermann, W., Asmi, A., Fuzzi, S., and Facchini, M. C.: Cloud condensation nucleus production from nucleation events at a highly polluted region, Geophys. Res. Lett., 32, L06812, doi:10.1029/2004GL022092, 2005. 8918, 8929, 8935, 8937

Lihavainen, H., Kerminen, V.-M., Komppula, M., Hatakka, J., Aaltonen, V., Kulmala, M., and Viisanen, Y.: Production of "potential" cloud condensation nuclei associated with atmospheric new-particle formation in northern Finland, J. Geophys. Res., 108, 4782, doi:10.1029/2003JD003887, D24, 2003. 8917

Lohmann, U., Stier, P., Hoose, C., Ferrachat, S., Kloster, S., Roeckner, E., and Zhang, J.: Cloud microphysics and aerosol indirect effects in the global climate model ECHAM5-HAM, Atmos. Chem. Phys., 7, 3425–3446, doi:10.5194/acp-7-3425-2007, 2007.

Makkonen, R., Asmi, A., Korhonen, H., Kokkola, H., Järvenoja, S., Räisänen, P., Lehtinen, K. E. J., Laaksonen, A., Kerminen, V.-M., Järvinen, H., Lohmann, U., Bennartz, R., Feichter, J., and Kulmala, M.: Sensitivity of aerosol concentrations and cloud properties to nucleation and secondary organic distribution in ECHAM5-HAM global circulation model, Atmos. Chem. Phys., 9, 1747–1766, doi:10.5194/acp-9-1747-2009, 2009. 8918, 8924

Manninen, H. E., Nieminen, T., Asmi, E., Gagné, S., Häkkinen, S., Lehtipalo, K., Aalto, P., Vana, M., Mirme, A., Mirme, S., Hõrrak, U., Plass-Dülmer, C., Stange, G., Kiss, G., Hoffer, A., Törő, N., Moerman, M., Henzing, B., de Leeuw, G., Brinkenberg, M., Kouvarakis, G. N., Bougiatioti, A., Mihalopoulos, N., O'Dowd, C., Ceburnis, D., Arneth, A., Svenningsson, B., Swietlicki, E., Tarozzi, L., Decesari, S., Facchini, M. C., Birmili, W., Sonntag, A., Wiedensohler, A., Boulon, J., Sellegri, K., Laj, P., Gysel, M., Bukowiecki, N., Weingartner, E., Wehrle, G., Laaksonen, A., Hamed, A., Joutsensaari, J., Petäjä, T., Kerminen, V.-M., and Kulmala, M.: EUCAARI ion spectrometer measurements at 12 European sites – analysis of new particle formation events, Atmos. Chem. Phys., 10, 7907–7927, doi:10.5194/acp-10-7907-2010, 2010. 8949

Matsui, H., Koike, M., Kondo, Y., Takegawa, N., Wiedensohler, A., Fast, J. D., and Zaveri, R. A.: Impact of new particle formation on the concentrations of aerosols and cloud condensation nuclei around Beijing, J. Geophys. Res., 116, D19208, doi:10.1029/2011JD016025, 2011. 8919

Merikanto, J., Zapadinsky, E., Lauri, A., and Vehkamäki, H.: Origin of the failure of classical nucleation theory: incorrect description of the smallest clusters, Phys. Rev. Lett., 98, 145702, doi:10.1103/PhysRevLett.98.145702, 2007. 8918

ACPD
14, 8915–8961, 2014

Merikanto, J., Spracklen, D. V., Mann, G. W., Pickering, S. J., and Carslaw, K. S.: Impact of nucleation on global CCN, Atmos. Chem. Phys., 9, 8601–8616, doi:10.5194/acp-9-8601-2009, 2009. 8919

Mikkonen, S., Romakkaniemi, S., Smith, J. N., Korhonen, H., Petäjä, T., Plass-Duelmer, C., Boy, M., McMurry, P. H., Lehtinen, K. E. J., Joutsensaari, J., Hamed, A., Mauldin III, R. L., Birmili, W., Spindler, G., Arnold, F., Kulmala, M., and Laaksonen, A.: A statistical proxy for sulphuric acid concentration, Atmos. Chem. Phys., 11, 11319–11334, doi:10.5194/acp-11-11319-2011, 2011. 8922

Modgil, M. S., Kumar, S., Tripathi, S. N., and Lovejoy, E. R.: A parameterization of ion-induced nucleation of sulphuric acid and water for atmospheric conditions, J. Geophys. Res., 110, D19205, doi:10.1029/2004JD005475, 2005. 8918

Napari, I., Noppel, M., Vehkamäki, H., and Kulmala, M.: Parametrization of ternary nucleation rates for H_2SO_4-NH_3-H_2O vapors, J. Geophys. Res., 107, 4381, doi:10.1029/2002JD002132, 2002. 8918

O'Dowd, C. D., Hämeri, K., Mäkelä, J., Väkeva, M., Aalto, P., de Leeuw, G., Kunz, G. J., Becker, E., Hansson, H.-C., Allen, A. G., Harrison, R. M., Berresheim, H., Kleefeld, C., Geever, M., Jennings, S. G., and Kulmala, M.: Coastal new particle formation: environmental conditions and aerosol physicochemical characteristics during nucleation bursts, J. Geophys. Res., 107, 8107, doi:10.1029/2000JD000206, 2002. 8930

Petäjä, T., Mauldin, III, R. L., Kosciuch, E., McGrath, J., Nieminen, T., Paasonen, P., Boy, M., Adamov, A., Kotiaho, T., and Kulmala, M.: Sulfuric acid and OH concentrations in a boreal forest site, Atmos. Chem. Phys., 9, 7435–7448, doi:10.5194/acp-9-7435-2009, 2009. 8923

Pfeifer, S.: Modeling cold cloud processes with the regional climate model REMO, Ph.D. thesis, Reports on Earth System Science, Max Planck Institute for Meteorology, Hamburg, 2006. 8921

Pierce, J. R. and Adams, P. J.: Uncertainty in global CCN concentrations from uncertain aerosol nucleation and primary emission rates, Atmos. Chem. Phys., 9, 1339–1356, doi:10.5194/acp-9-1339-2009, 2009. 8919

Pierce, J. R., Chen, K., and Adams, P. J.: Contribution of primary carbonaceous aerosol to cloud condensation nuclei: processes and uncertainties evaluated with a global aerosol microphysics model, Atmos. Chem. Phys., 7, 5447–5466, doi:10.5194/acp-7-5447-2007, 2007. 8919

ACPD
14, 8915–8961, 2014

Pietikäinen, J.-P., O'Donnell, D., Teichmann, C., Karstens, U., Pfeifer, S., Kazil, J., Podzun, R., Fiedler, S., Kokkola, H., Birmili, W., O'Dowd, C., Baltensperger, U., Weingartner, E., Gehrig, R., Spindler, G., Kulmala, M., Feichter, J., Jacob, D., and Laaksonen, A.: The regional aerosol-climate model REMO-HAM, Geosci. Model Dev., 5, 1323–1339, doi:10.5194/gmd-5-1323-2012, 2012. 8920, 8921, 8924, 8927, 8929, 8933, 8934, 8938

Pikridas, M., Riipinen, I., Hildebrandt, L., Kostenidou, E., Manninen, H., Mihalopoulos, N., Kalivitis, N., Burkhart, J. F., Stohl, A., Kulmala, M., Pandis, S. N.: New particle formation at a remote site in the eastern Mediterranean, J. Geophys. Res., 117, D12205, doi:10.1029/2012JD017570, 2012. 8949

Pirjola, L., Lehtinen, K. E. J., Hansson, H.-C., and Kulmala, M.: How important is nucleation in regional/global modelling?, Geophys. Res. Lett., 31, L12109, doi:10.1029/2004GL019525, 2004.

Rechid, D.: Land Surface Scheme of REMO, Internal report, Max Planck Institute for Meteorology, Hamburg, 3 pp., available at: http://www.remo-rcm.de/fileadmin/user_upload/remo/UBA/pdf/LandSurfaceScheme_REMO_short-summary.pdf (last access: 1 March 2014), 2009. 8921

Roeckner, E., Arpe, K., Bengtsson, L., Christoph, M., Claussen, M., Dumenil, L., Esch, M., Schlese, U., and Schulzweida, U.: The atmospheric general circulation model ECHAM4: Model description and simulation of present-day climate, Max Planck Institute for Meteorology report series, Hamburg, Germany, Report No. 218, 1996. 8921

Roeckner, E., Baeuml, G., Bonventura, L., Brokopf, R., Esch, M., Giorgetta, M., Hagemann, S., Kirchner, I., Kornblueh, L., Manzini, E., Rhodin, A., Schlese, U., Schulzweida, U., and Tompkins, A.: The atmospheric general circulation model ECHAM5. PART I: Model description, Max Planck Institute for Meteorology report series, Hamburg, Germany, Report No. 349, 2003. 8920

Rohrer, F. and Berresheim, H.: Strong correlation between levels of tropospheric hydroxyl radicals and solar ultraviolet radiation, Nature, 442, 184–187, doi:10.1038/nature04924, 2006. 8922

Seinfeld, J. and Pandis, S.: Atmospheric Chemistry and Physics, John Wiley & Sons inc., New York, 1998. 8922

Semmler, T., Jacob, D., Schlünzen, K. H., and Podzun, R.: Influence of sea ice treatment in a regional climate model on boundary layer values in the Fram Strait region, Mon. Weather Rev., 132, 985–999, 2004. 8921

ACPD
14, 8915–8961, 2014

Sihto, S.-L., Kulmala, M., Kerminen, V.-M., Dal Maso, M., Petäjä, T., Riipinen, I., Korhonen, H., Arnold, F., Janson, R., Boy, M., Laaksonen, A., and Lehtinen, K. E. J.: Atmospheric sulphuric acid and aerosol formation: implications from atmospheric measurements for nucleation and early growth mechanisms, Atmos. Chem. Phys., 6, 4079–4091, doi:10.5194/acp-6-4079-2006, 2006. 8918

Sotiropoulou, R. E. P., Tagaris, E., Pilinis, C., Anttila, T., and Kulmala, M.: Modeling new particle formation during air pollu- tion episodes: impacts on aerosol and cloud condensation nuclei, Aerosol Sci. Tech., 40, 557–572, 2006. 8919

Spracklen, D. V., Carslaw, K. S., Kulmala, M., Kerminen, V.-M., Sihto, S.-L., Riipinen, I., Merikanto, J., Mann, G. W., Chipperfield, M. P., Wiedensohler, A., Birmili, W., and Lihavainen, H.: The contribution of particle formation to global cloud condensation nuclei concentrations, Geophys. Res. Lett., 35, L06808, doi:10.1029/2007GL033038, 2008. 8918

Stier, P., Feichter, J., Kinne, S., Kloster, S., Vignati, E., Wilson, J., Ganzeveld, L., Tegen, I., Werner, M., Balkanski, Y., Schulz, M., Boucher, O., Minikin, A., and Petzold, A.: The aerosol-climate model ECHAM5-HAM, Atmos. Chem. Phys., 5, 1125–1156, doi:10.5194/acp-5-1125-2005, 2005. 8920, 8921

Trivitayanurak, W., Adams, P. J., Spracklen, D. V., and Carslaw, K. S.: Tropospheric aerosol microphysics simulation with assimilated meteorology: model description and intermodel comparison, Atmos. Chem. Phys., 8, 3149–3168, doi:10.5194/acp-8-3149-2008, 2008. 8919

Vehkamäki, H., Kulmala, M., Napari, I., Lehtinen, K. E. J., Timmreck, C., Noppel, M., and Laaksonen, A.: An improved parameterization for sulfuric acid-water nucleation rates for tropospheric and stratospheric conditions, J. Geophys. Res., 107, 4622, doi:10.1029/2002JD002184, 2002. 8918, 8923

Vignati, E., Wilson, J., and Stier, P.: M7: an efficient size-resolved aerosol microphysics module for large-scale aerosol transport models, J. Geophys. Res., 109, D22202, doi:10.1029/2003JD004485, 2004. 8920

Wang, M. and Penner, J. E.: Aerosol indirect forcing in a global model with particle nucleation, Atmos. Chem. Phys., 9, 239–260, doi:10.5194/acp-9-239-2009, 2009. 8919

Yoon, Y. J., O'Dowd, C. D., Jennings, S. G., and Lee, S. H.: Statistical characteristics and predictability of particle formation events at Mace Head, J. Geophys. Res., 111, D13204, doi:10.1029/2005JD006284, 2006. 8929, 8930, 8949

ACPD
14, 8915–8961, 2014

Yu, F. and Luo, G.: Simulation of particle size distribution with a global aerosol model: contribution of nucleation to aerosol and CCN number concentrations, Atmos. Chem. Phys., 9, 7691–7710, doi:10.5194/acp-9-7691-2009, 2009. 8919

Zhang, K., O'Donnell, D., Kazil, J., Stier, P., Kinne, S., Lohmann, U., Ferrachat, S., Croft, B., Quaas, J., Wan, H., Rast, S., and Feichter, J.: The global aerosol-climate model ECHAM-HAM, version 2: sensitivity to improvements in process representations, Atmos. Chem. Phys., 12, 8911–8949, doi:10.5194/acp-12-8911-2012, 2012. 8920

ACPD
14, 8915–8961, 2014

Table 1. Measurement sites with long-term observations of the new particle formation events analysed in this work.

Observation site	Coordinates	Altitude (m a.s.l.)	Measurement period	Reference
Hyytiälä, Finland	61°50′ N, 24°18′ E	181	1 Jan 2003–31 Dec 2004 Mar 2008–Apr 2009	Hari and Kulmala (2005) Manninen et al. (2010)
Melpitz, Germany	51°32′ N, 12°54′ E	87	1 Jul 2003–31 Dec 2004 May 2008–Apr 2009	Birmili and Wiedensohler (2000) Engler et al. (2007) Manninen et al. (2010)
San Pietro Capofiume, Italy	44°37′ N, 11°40′ E	11	2003–Aug 2004 (partly Oct) Mar 2008–Sep 2008	Jaatinen et al. (2009) Manninen et al. (2010)
Mace Head, Ireland	53°19′ N, 09°53′ E	5	Aug 2002–Jul 2004 Jun 2008–Apr 2009	Yoon et al. (2006) Manninen et al. (2010)
Hohenpeißenberg, Germany	47°48′ N, 11°00′ E	985	Apr 1998–Aug 2000 Apr 2008–Apr 2009	Birmili et al. (2003) Manninen et al. (2010)
Värriö, Finland	67°46′ N, 29°35′ E	400	2003–2004	Dal Maso et al. (2007)
Pallas, Finland	67°58′ N, 24°07′ E	560	2003–2004 Apr 2008–Apr 2009	Dal Maso et al. (2007) Manninen et al. (2010)
Vavihill, Sweden	56°01′ N, 13°09′ E	172	Feb 2001–May 2004 Apr 2008–Feb 2009	Kristensson et al. (2011) Manninen et al. (2010)
Finokalia, Greece	35°20′ N, 25°40′ E	250	Apr 2008–Apr 2009 Apr 2008–Apr 2009	Pikridas et al. (2012) Manninen et al. (2010)
Cabauw, Netherlands	51°57′ N, 04°53′ E	0	Apr 2008–Mar 2009	Manninen et al. (2010)
K-Puszta, Hungary	46°58′ N, 19°35′ E	125	Mar 2008–Feb 2009	Manninen et al. (2010)
Puy de Dôme, France	45°42′ N, 03°13′ E	1465	Feb 2007–Jun 2010 Apr 2008–Apr 2009	Boulon et al. (2011) Manninen et al. (2010)
Jungfraujoch, Switzerland	46°32′ N, 07°57′ E	3580	Apr 2008–Apr 2009 Apr 2008–Apr 2009	Boulon et al. (2010) Manninen et al. (2010)

ACPD
14, 8915–8961, 2014

Table 2. Annual production of nucleated 3 nm particles in the boundary layer.

Year	SPC [#m^{-2}]	Europe (land points) [# m^{-2}]
2003	2.4×10^{15}	2.0×10^{15}
2004	2.1×10^{15}	1.7×10^{15}
2008	2.3×10^{15}	1.9×10^{15}
2009	2.3×10^{15}	1.9×10^{15}

ACPD
14, 8915–8961, 2014

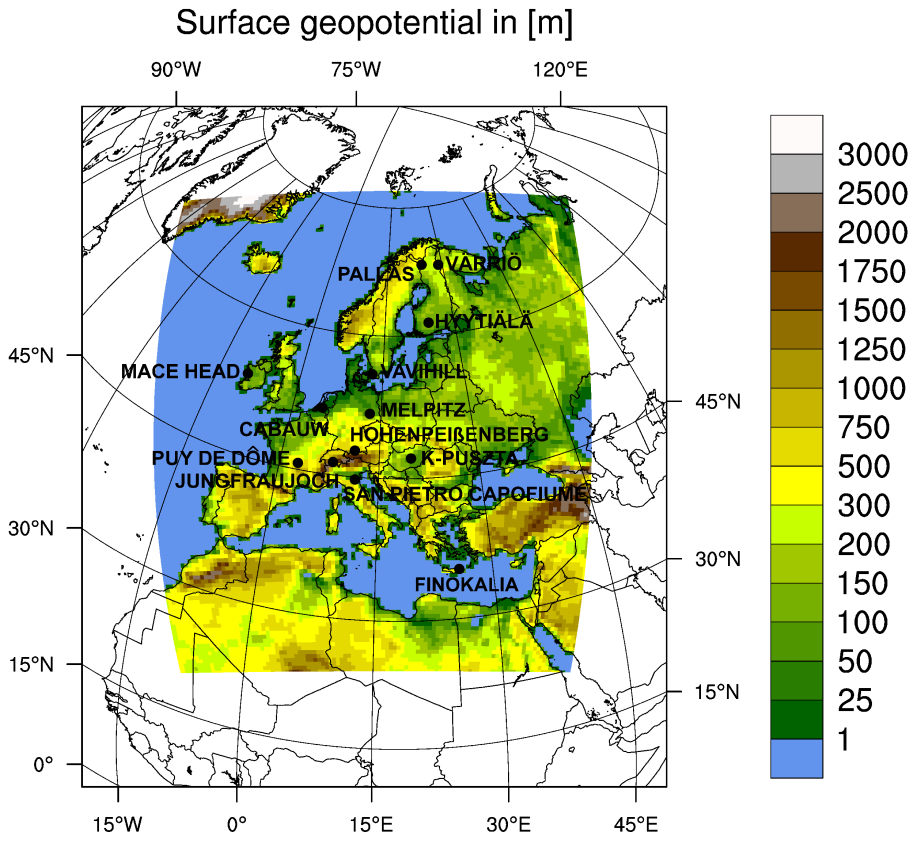

Fig. 1. The orography of the REMO domain and the analysed locations.

ACPD
14, 8915–8961, 2014

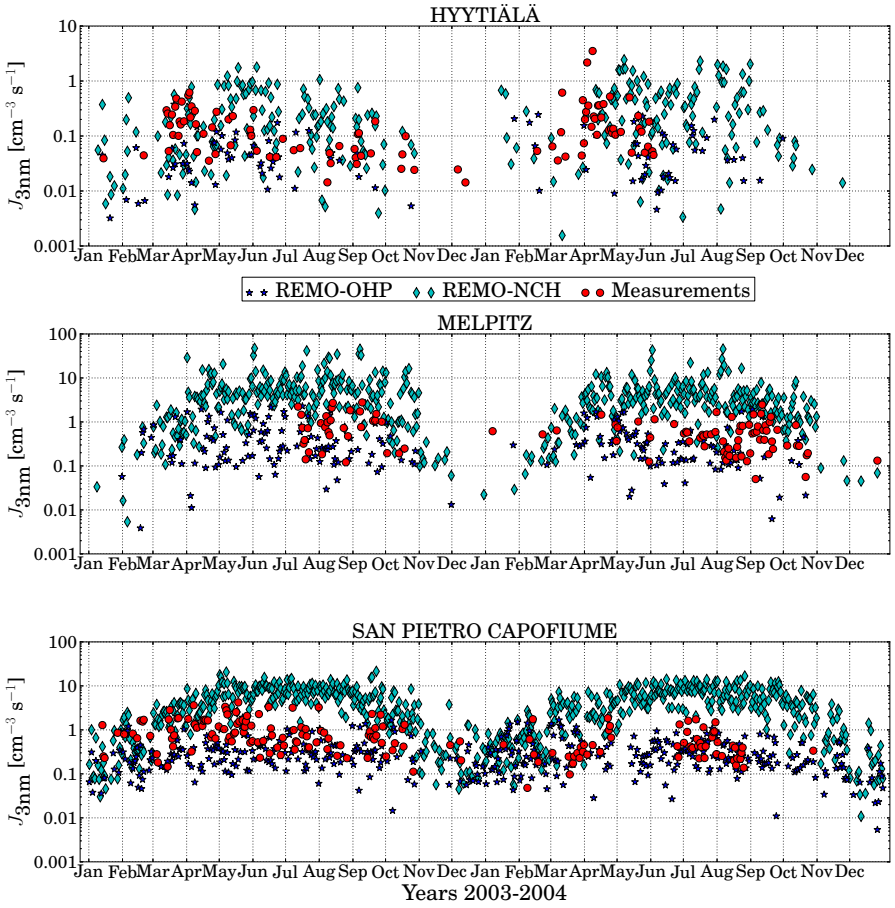

Fig. 2. Measured and modelled daily mean J_{3nm} rates for event days at Hyytiälä, Melpitz and San Pietro Capofiume.

ACPD
14, 8915–8961, 2014

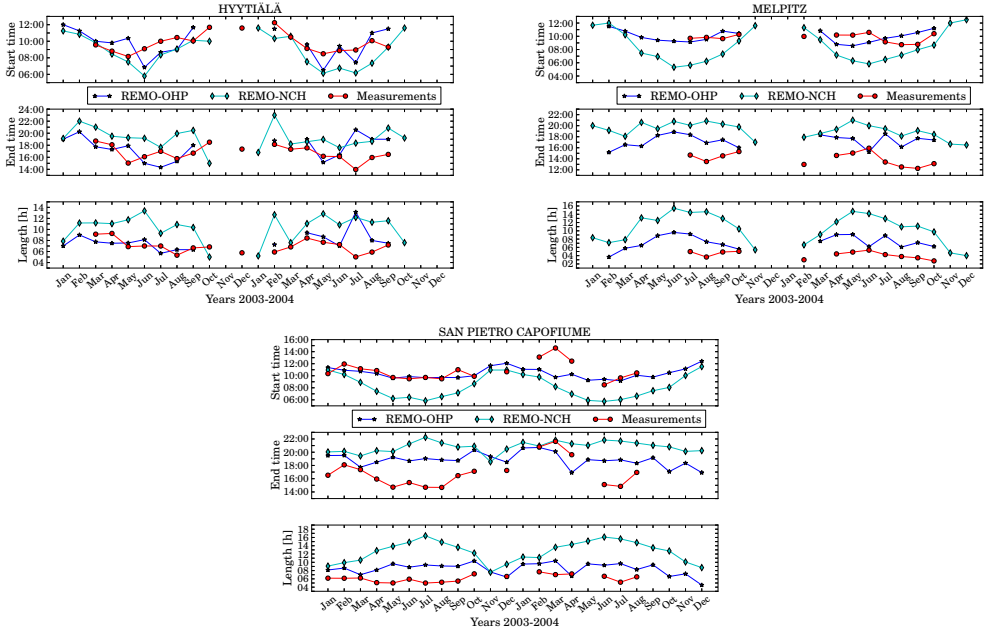

Fig. 3. Monthly mean event start time, end time and length at Hyytiälä, Melpitz and San Pietro Capofiume. Months without data or events have been dismissed.

ACPD
14, 8915–8961, 2014

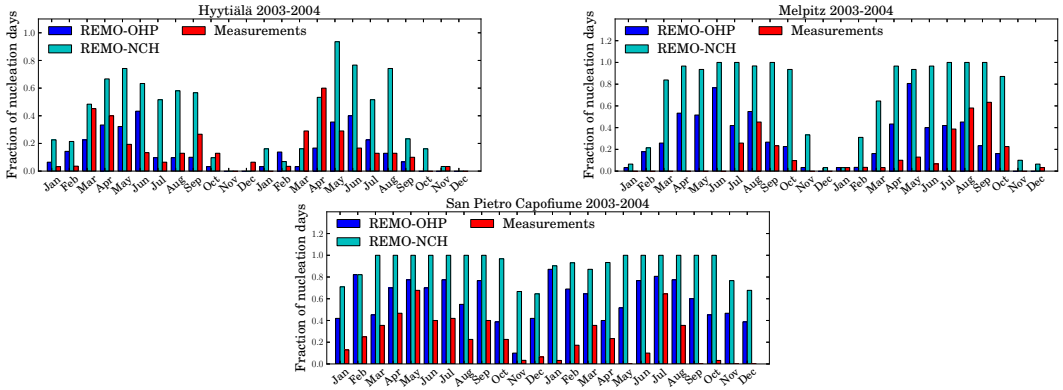

Fig. 4. The fraction of days with NPF events, 2003–2004, at 3 European observation sites on a monthly basis. The graph compares model simulations with observational evidence.

ACPD
14, 8915–8961, 2014

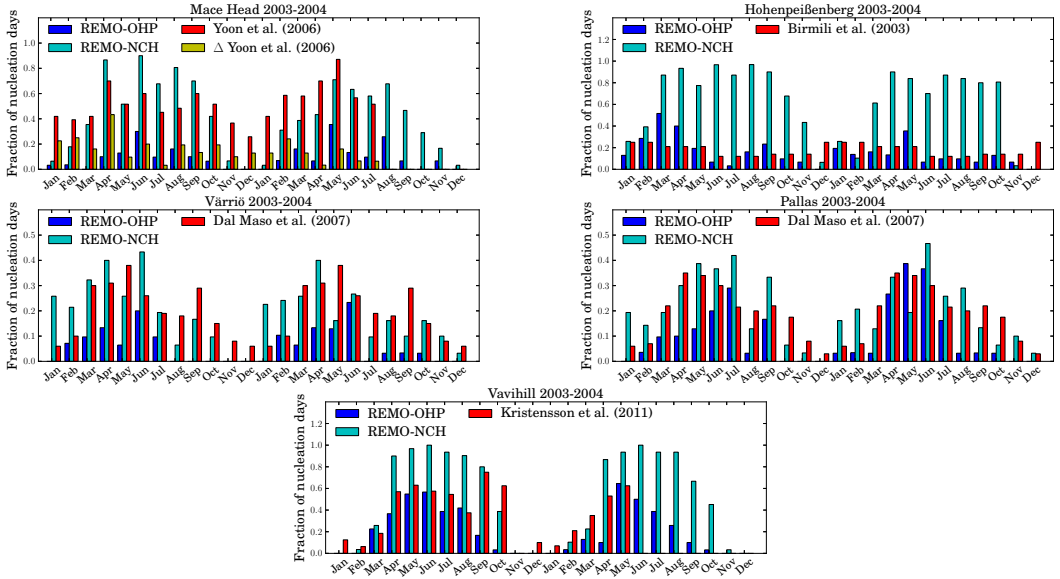

Fig. 5. The fraction of days with NPF events, 2003–2004, at 5 European observation sites on a monthly basis.

ACPD
14, 8915–8961, 2014

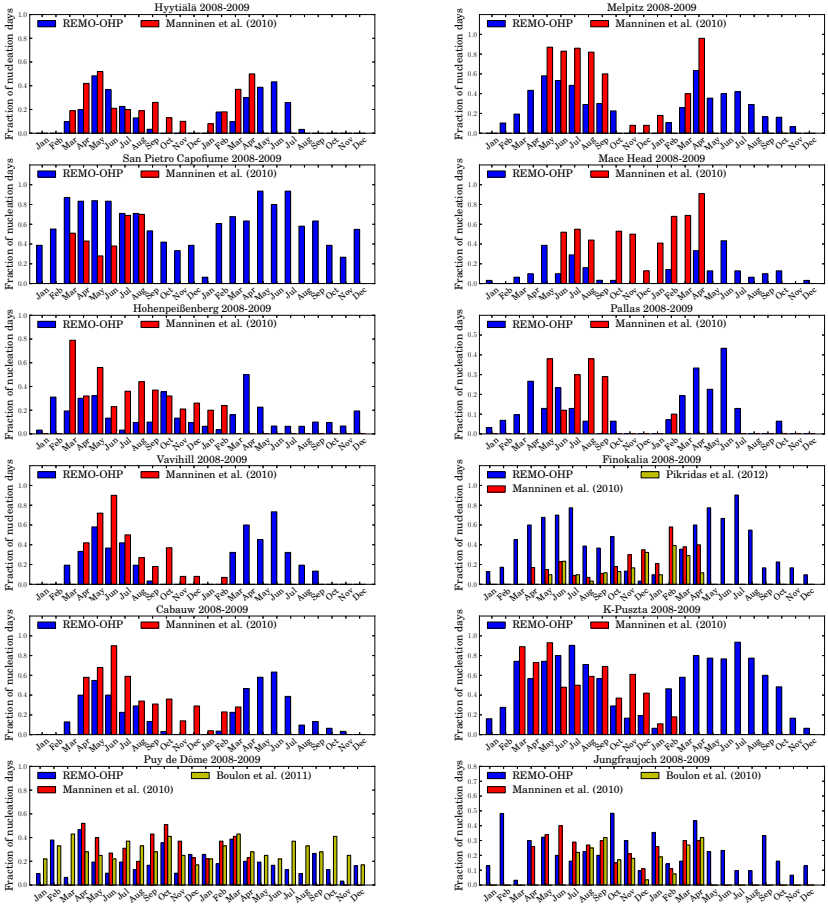

Fig. 6. The fraction of days with NPF events, 2008–2009, at 12 European observation sites on a monthly resolution.

ACPD
14, 8915–8961, 2014

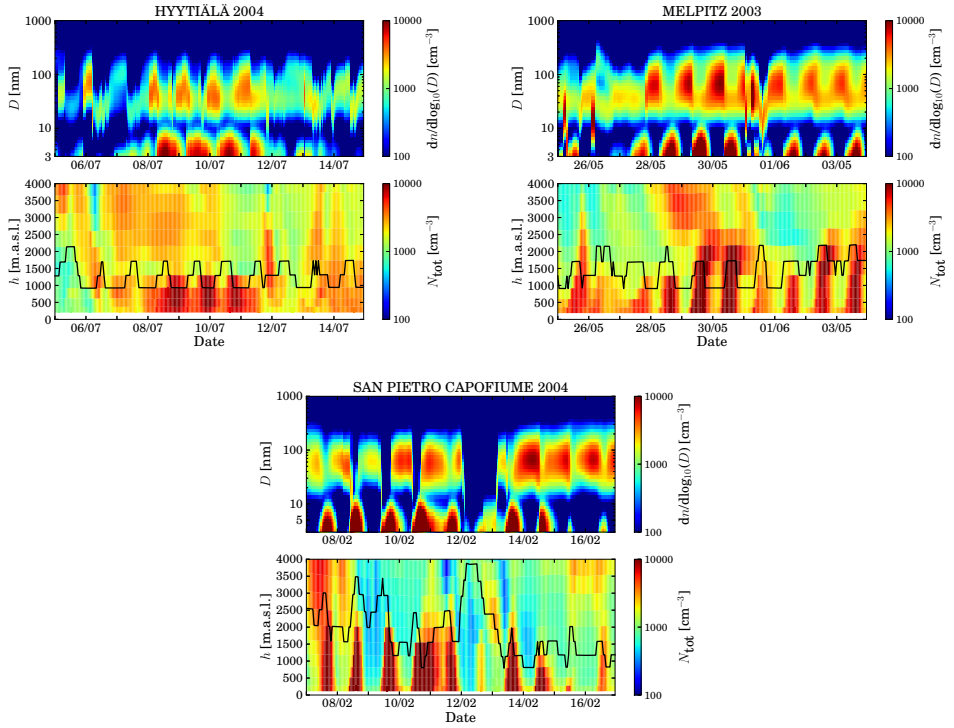

Fig. 7. Nucleation events and total number concentration from Hyytiälä (5 to 15 July 2004), Melpitz (25 May to 4 June 2003) and San Pietro Capofiume (7 to 17 February 2004). The black line shows the height of the boundary layer.

ACPD
14, 8915–8961, 2014

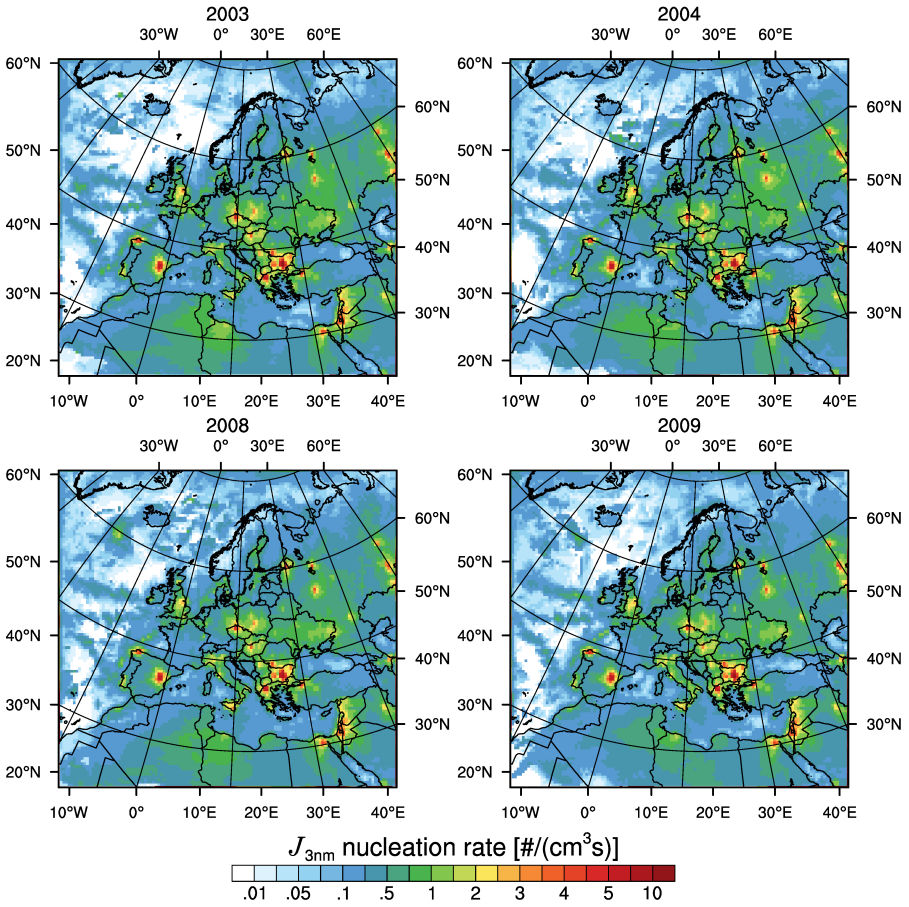

Fig. 8. The yearly mean nucleation rates. Means are calculated only for data that meets the event classification criteria presented in Sect. 3.3.

ACPD
14, 8915–8961, 2014

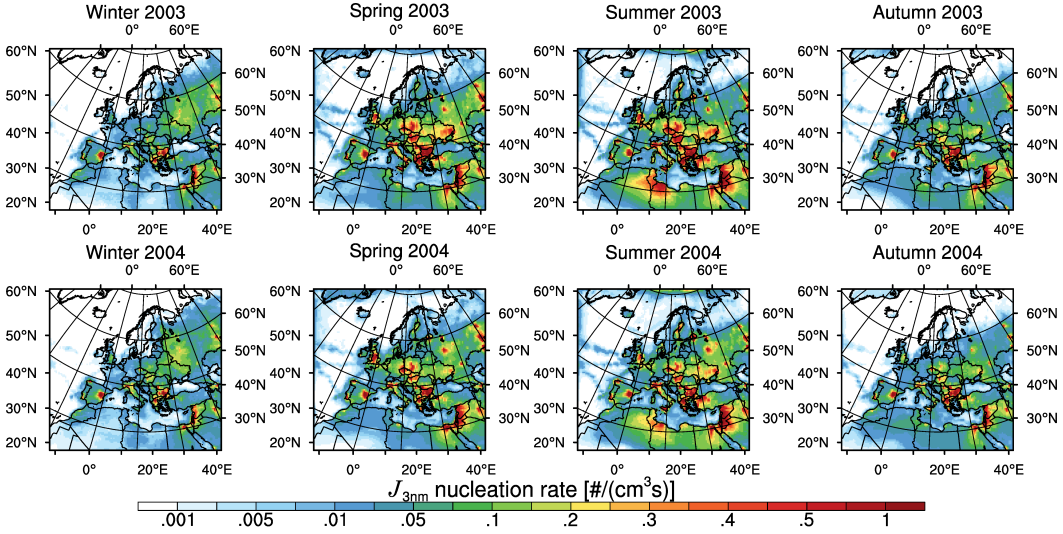

Fig. 9. The seasonal mean nucleation rates for 2003 and 2004.

ACPD
14, 8915–8961, 2014

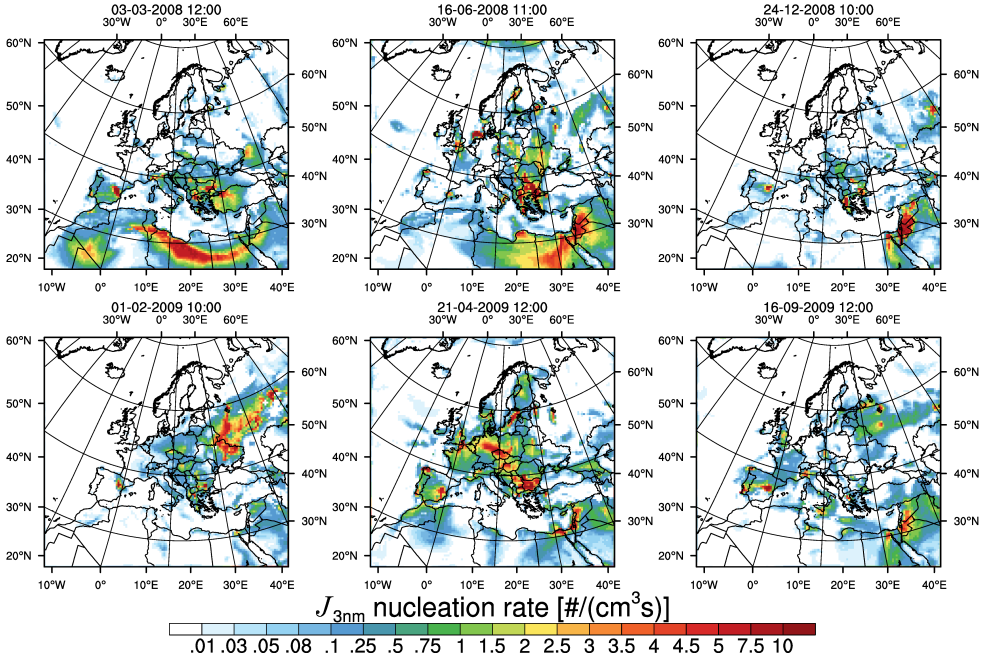

Fig. 10. Snapshot examples of 6 different European nucleation events.

ACPD
14, 8915–8961, 2014

Modelling European boundary layer nucleation

J.-P. Pietikäinen

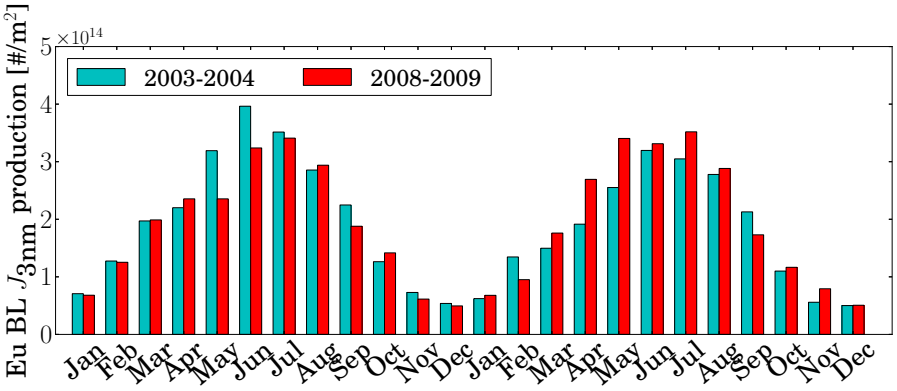

Fig. 11. Monthly nucleated 3 nm particle burden calculated only for the boundary layer.

ACPD
14, 8915–8961, 2014